Microgravity Science and Technology (2019) 31:603–613
https://doi.org/10.1007/s12217-019-09731-9

ORIGINAL ARTICLE

Condensation on Composite V-Shaped Surface with Different Gravity in Nanoscale

Bo Xu[1] · Zhenqian Chen[1,2,3]

Received: 25 December 2018 / Accepted: 10 July 2019 / Published online: 3 August 2019
© Springer Nature B.V. 2019

Abstract

The model of water vapor condensation on a composite V-shaped surface with multi wettability gradients was built and the condensation process with different gravity was studied by molecular dynamics to find out whether this model could control the condensation mode and accelerate the condensate drainage from the micro-perspective. With the absence of gravity, the simulation results indicated that the condensation mode could be controlled as a dropwise condensation. What's more, the movement of condensate nano-droplet also could be controlled, which was helpful for increasing the efficiency of condensate drainage. The temperature of hot wall was largest while it was smallest for cold wall. The temperature of water was in the middle. The result was in accordance with the law of energy conservation. However, the condensation process was different with the effect of gravity. It can be concluded that the condensation process was much quicker with greater gravity, leading to the larger condensation rate. The temperature of cold wall and water were larger than that of hot wall, especially for greater gravity. It was because the part of energy generated by gravity transferred to the thermal energy of water and cold wall, and the other part transferred to the kinetic energy of water. The gravitational potential energy and kinetic energy increased with greater gravity, while the thermal energy increased first and then decreased, corresponding well with the final temperature of condensation process with different gravity. The results will provide a microcosmic mechanism for space experiment and guidance for space system drainage.

Keywords Dropwise condensation · V-shaped surface · Gravity · Temperature · Energy

Introduction

Recent decades, many scholars' attention was attracted by phase change process with altered gravity to improve the heat transfer in space applications (Legros et al. 2018a; Legros et al. 2018b; Glushkov et al. 2016; Lei et al. 2017). In addition, as a main representative of phase change process, condensation was quite important and widely applied in space system. Lin (Lin and Hudman 1995) theoretically studied an exact solution of a differential system for non-equilibrium evaporation or condensation under weightless conditions across an interface and obtained the functional relations between relevant parameters and the evaporation coefficient which appeared in the theory of non-equilibrium evaporation or condensation. Zhang (Zhang et al. 2018) experimentally proposed a new type of three-dimensional pin-fin plate with elliptical cross-section. With the increase of inclination angle, the gravity effect in the direction of condensate flow decreased, resulting in the deterioration of heat transfer. Pu (Pu et al. 2009) adopted a level set method being coupled with the moving mesh method in the double-staggered grid systems to study the two-phase flows including phase change under microgravity conditions. The results indicated that condensation process under the normal gravity condition was different from it under microgravity conditions. Finally, when condensation kept going, the condensed liquid was needed to drain away quickly.

This article belongs to the Topical Collection: Thirty Years of Microgravity Research - A Topical Collection Dedicated to J. C. Legros Guest Editor: Valentina Shevtsova

✉ Zhenqian Chen
zqchen@seu.edu.cn

[1] School of Energy and Environment, Southeast University, Nanjing, People's Republic of China

[2] Jiangsu Provincial Key Laboratory of Solar Energy Science and Technology, School of Energy and Environment, Southeast University, Nanjing, People's Republic of China

[3] Key Laboratory of Energy Thermal Conversion and Control of Ministry of Education, School of Energy and Environment, Southeast University, Nanjing, People's Republic of China

Many organisms possess special surface structures with unique wettability and shapes for water collection automatically. For example, cactus spines are found to have high efficiency of fog collection and self-driven process of droplet on cactus spines is investigated (Parker and Lawrence 2001). A wettability gradient of micro- and nanostructure is formed along the exterior surface of papilla of lotus leaf including nanohairs during water condensation, leading to a tendency of directional movement and enabling the micro droplet moving out of the valley of papillae (Zheng et al. 2008; Cheng et al. 2005). Desert beetles used micrometer-sized patterns of hydrophobic and hydrophilic regions on their backs to capture water from humid air (Zheng et al. 2010; Chen and Zheng 2014). Controlled self-propelling of droplet has an extensive application prospect in many fields (Gau et al. 1999; ElSherbini and Jacobi 2005; Idem et al. 2000), such as fog-harvesting, microfluidic device, condensing apparatus and industrial filtration equipment. What's more, it could be widely used for electron component and cooling system of spacecraft.

Molecular dynamics (MD) simulation is widely used to study the interactions including vapor condensation in microscale with the rapid development of computational capabilities. The concept of molecular clustering has been introduced to explain the formation mechanism of initial droplets (Song et al. 2009) and the nucleation process has been investigated using MD simulation (Yasuoka and Matsumoto 1998a; Yasuoka and Matsumoto 1998b; Jung et al. 2016; Wolde and Frenkel 1998; Diemand et al. 2013; Yasuoka et al. 2000; Toxværd 2002). For example, Wolde (Wolde and Frenkel 1998) reported a computer-simulation study of homogeneous gas-liquid nucleation in a Lennard-Jones system and illustrated that mechanical surface tension and thermodynamical surface tension were significantly different. Zheng (Li et al. 2009) observed a condensation phenomenon in free expansion plumes and developed a model of water cluster sizes, cluster-monomer collisions, and sticking probabilities necessary for studying water homogeneous condensation in a plume expanding to low pressure, space conditions. Gao (Gao et al. 2017) performed the dynamic wetting behavior of water droplets and condensation process of water molecules on substrates with different pillar structure parameters by molecular dynamic simulation. Therefore, MD was quite suitable to study the mechanism and behavior of condensation on a controlled surface with different gravity in microscale.

In this work, MD simulation was used to study the condensation of droplet on V-shaped surface with different gravity. Different gravity was investigated to fulfill the condensation on horizontal surface to extend our understandings about the mechanism of space condensation.

Models and Methods

All of molecular dynamics simulations were carried out by LAMMPS package (Plimpton 1995). The relationship between wettability of solid surface with ε_{cu-o} (The potential between copper atom and oxygen atom of water droplet) was described in detail in our previous work (Xu and Chen 2018; Xu and Chen 2019) and the correlations were shown in Fig. 1. The TIP3P water model (Price et al. 1984) was employed containing a single Lennard-Jones center. Water molecule had three charges, including −0.834e for oxygen atom and + 0.417e for hydrogen atoms with an angle of 104.52°between oxygen and hydrogen atoms. The bond distance and angle of the water molecules are fixed using the Shake algorithm as a rigid-body water model. The ε_{o-o} and σ_{o-o} in water molecules are 0.1521 kcal/mol and 3.1507 Å respectively. The atoms of copper-type surface are fixed to their lattice sites, which can provide a realistic model of a solid surface (De Coninck and Blake 2008).

The model of water condensation containing 8340 water molecules and 85440 copper-type atoms was built in Fig. 2 to investigate the effect of different gravity. The cold wall was in the size of 252.7 Å × 151.62 Å × 10.83 Å for direction of $x \times y \times z$. The length and bottom of V-shaped surface was 162.45 Å and 14.44 Å. The distance between cold wall and hot wall was 101.08 Å. The width and thickness of hot wall were the same to cold wall, while the length of hot wall was 198.55 Å. In addition, the brown atoms were set as a wall to prevent water vapor molecules from crossing borders and the thickness of all brown walls were 1.805 Å. The interaction between water molecules and brown copper-types atoms were 0, thus the water molecule rebounding from brown walls. For the hot walls, the outside two layers of copper-type atoms were kept fixed to avoid the deformation of the solid wall and the next two layers were treated as heating source. The inside two layers of copper-type atoms were built to exchange energy between the water molecules and heating source. Such a setting was adopted to build the heating surface in previous studies (Hens et al. 2014; Fu et al. 2015; Seyf and Zhang 2013) and has been proved to effectively avoid artificial thermal resistance caused by the applied thermostat (Barisik and Beskok 2012). However, for the cold walls, the outside two layers of copper-type atoms were kept fixed to avoid the deformation of the solid wall and the inside four layers were built to exchange energy between the water molecules and cold wall. With these settings, the condensation process and temperature change of cold surface without a fixed cold source were simulated and studied. The whole simulation time is 1600 ps with a time step of 2 fs. The first 100 ps was to obtain the two phase equilibrium of water vapor with NVT (Number of atoms, Volume and Temperature are constant) ensemble using Nose-Hoover thermostat (Hoover 1985) at 298 K for all atoms. Then during the next 1500 ps period for

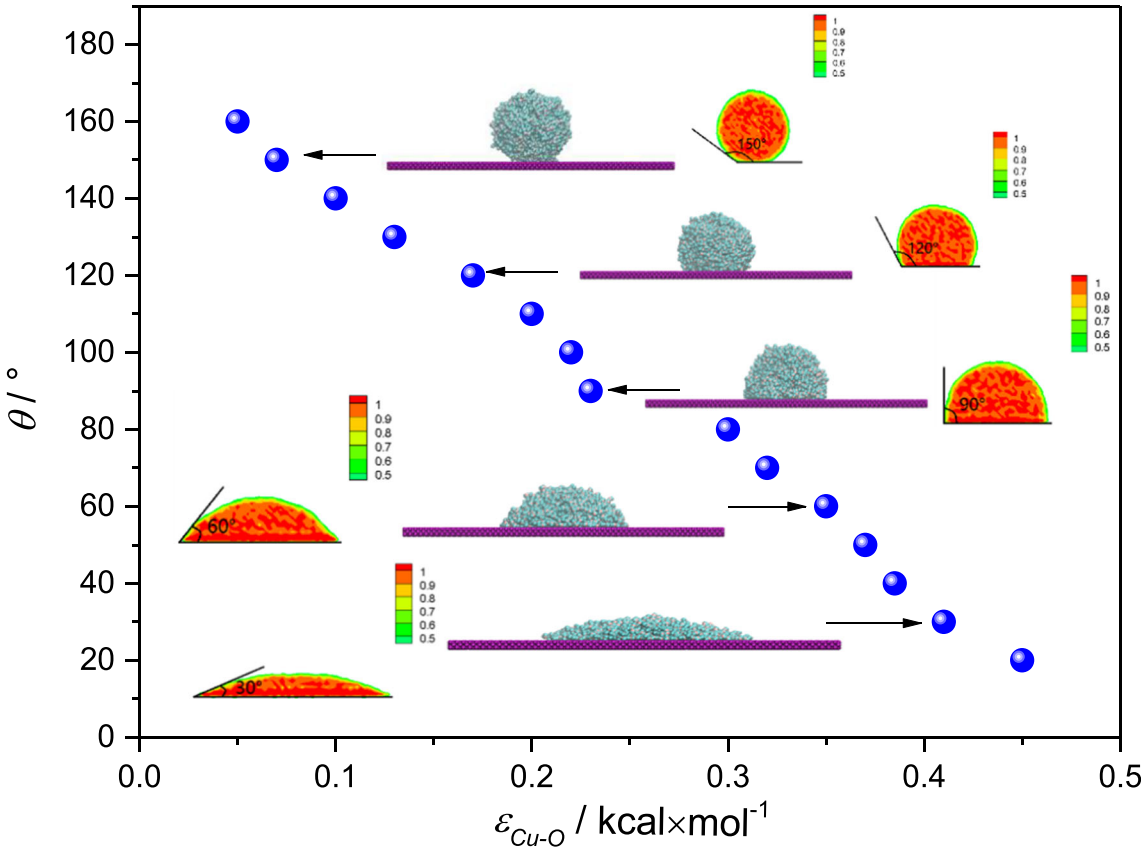

Fig. 1 Correlations of contact angle (θ) with ε_{Cu-O}

condensation, NVE (Number of atoms, Volume and Energy are constant) ensemble was applied on water molecules and copper atoms of cold wall, while the NVT ensemble was still applied for hot wall and the temperature of hot wall increased to 498 K. The water vapor of hot wall with high temperature began to evaporate and then condensed on the cold surface. The long-range electrostatic interactions are calculated using the PPPM (particle-particle particle-mesh) method. The periodic boundary condition is applied in all three spatial dimensions of the simulation box. Newton's equation of motion is integrated numerically using the velocity Verlet algorithm.

The interaction between the water and copper-type surface is also assumed to be 12–6 Lennard-Jones (LJ) particles (Alexiadis and Kassinos 2008) as follow:

$$U_{ij}(r_{ij}) = 4\varepsilon_{ij}\left[\left(\frac{\sigma_{ij}}{r_{ij}}\right)^{12} - \left(\frac{\sigma_{ij}}{r_{ij}}\right)^{6}\right] \quad (1)$$

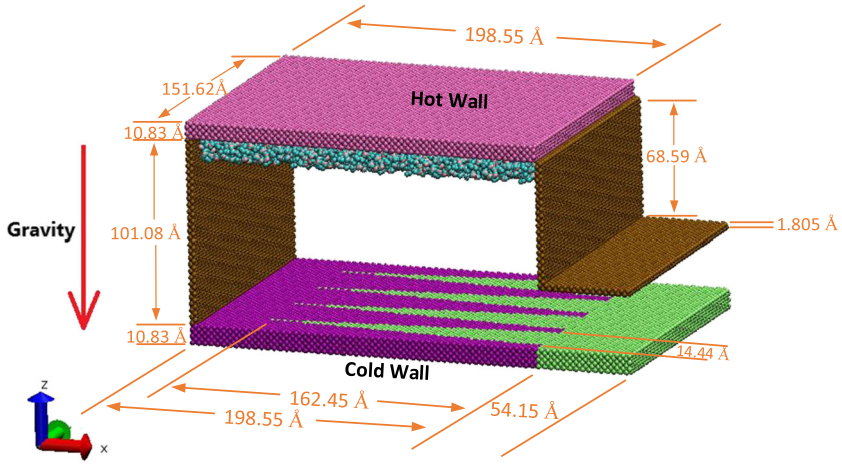

Fig. 2 Model of water vapor condensation in different gravity

$$\varepsilon_{ij} = \sqrt{\varepsilon_i \varepsilon_j} \quad (2)$$

$$\sigma_{ij} = \frac{(\sigma_i + \sigma_j)}{2} \quad (3)$$

where r_{ij}, ε_{ij} and σ_{ij} are the distance, well depth and equilibrium distance between a pair of atoms or charges. ε_{cu-o} can be used to tune the wettability of the copper-type surface. ε_{ij} and σ_{ij} between different species i and j are calculated by using Lorentz-Bertholet mixing rule. The cutoff distances for LJ and Coulomb interactions are 10 Å and 12 Å.

Contact angle was used to represent the wettability of copper-type surface. The purple copper-type atoms and green copper-type atoms represent $\theta = 120°$ and $\theta = 70°$ respectively. When applied microscale gravity (G) was smaller than 0.001 kcal/(mol·Å) (1 kcal/(mol·Å) = 2.33×10^{15} m/s^2), the condensation process and phenomena was similar to it without gravity. Therefore, The gravity changed from 0.001 kcal/(mol·Å) to 0.01 kcal/(mol·Å). The ratio (φ) of microscale gravity to normal macroscale gravity (g) was showed as followed: $\varphi = \frac{G}{g} = \frac{0.001 \text{ kcal}/(\text{mol}\cdot\text{Å})}{9.8 \text{ m/s}^2} = 2.38 \times 10^{11}$. The simulation model of Fig. 2 was similar to the case of water vapor condensation on horizontal plate in reality.

Results and Discussions

Condensation Process without Gravity

Phenomena of Condensation Process

The composite V-shaped surface with different wettability gradient without gravity was studied to discover whether such a surface could control the condensation mode and movement of condensate droplet. In order to investigate the phenomena more clearly, the condensation process was observed only less than 40 Å of z-axis, shown in Fig. 3.

The hydrophilic surface will attract more water vapor molecules due to the larger interaction between hydrophilic surface and water molecules than hydrophobic surface. Hence, the water vapor molecules rarely condensed on hydrophobic surface. The water vapor-liquid equilibrium obtained during the first 100 ps period. At 200 ps, there were no clusters or nuclei formed on copper-type surface because the condensation just began for 100 ps and the water molecules moved from the hot wall to nearby of cold wall. When it came to 400 ps, some clusters and nuclei appeared on hydrophilic surface ("□" at 400 ps). Since the vertex of V-shaped surface was the junction of two different wettability surfaces, the cluster first formed on the vertex of V-shaped surface. It was worth noting that the vertex of V-shaped surface is the activation center due to the interaction between two different wettability surfaces. Water molecules will preferentially condense in the activation center to form clusters (Shi et al. 1995). Then the clusters will move to the bottom. During the movement, some molecules condensed to the cluster directly and some clusters coalesced into each other to enlarge the cluster. At 500 ps, several nuclei formed on the each V-shaped surface and continued to move towards the bottom ("○" at 500 ps). With tine went on, the water nuclei attracted other clusters and molecules to enlarge themselves. At 800 ps, two main nano-droplets formed on the hydrophilic surface ("○" at 800 ps) and new cluster formed on the vertex of V-shaped surface ("□" at 800 ps). Then the new cluster enlarged to a nucleus and it kept moving to the bottom with the increase in volume ("○" at 1000 ps). Finally, it reached to the bottom and integrated into the nano-droplet. As the boundary condition of simulation box was periodic, actually at 1200 ps, only one nano-droplet survived because two nano-droplets coalesced with each other ("○" at 1200 ps). The clusters or nuclei formed by condensed water molecules continued moving to the bottom and merged into the nano-droplet, and the condensation process repeated over time. At last, all water vapor molecules will condense to form a nano-droplet at the bottom of V-shaped surface. It can be concluded that the condensation mode could be controlled as a dropwise condensation in this specific condition. Moreover, the movement of condensate nano-droplet also could be controlled, which was helpful for condensate drainage to increase the efficiency of condensate drainage.

Temperature of Condensation Process

It will take more time to obtain the stable state of condensation process without gravity, which can be seen clearly in Fig. 4. However, condensation phenomena was investigated and analyzed before 1600 ps because it was nearly the same after 1600 ps, greatly similar to condensation process with different gravity.

There were four key state points during the condensation process: ①Temperature change suddenly. At this moment, the temperature of hot wall increased to 498 K suddenly and two phase equilibrium will be broken. No water vapor molecule contacted cold wall. ② Water vapor molecules contacted cold wall. From this moment, the water vapor molecules began to contact the cold wall and transfer heat to cold wall, leading to the increase of cold wall temperature. However, since the contact time was too short for water molecules to grow up or coalesce with other molecules to form a cluster, no cluster formation was found, indicating that condensation has not occurred. ③ Condensation happened. From this moment, water clusters appeared on cold wall and water temperature became to equilibrium. With time went on, water molecules and

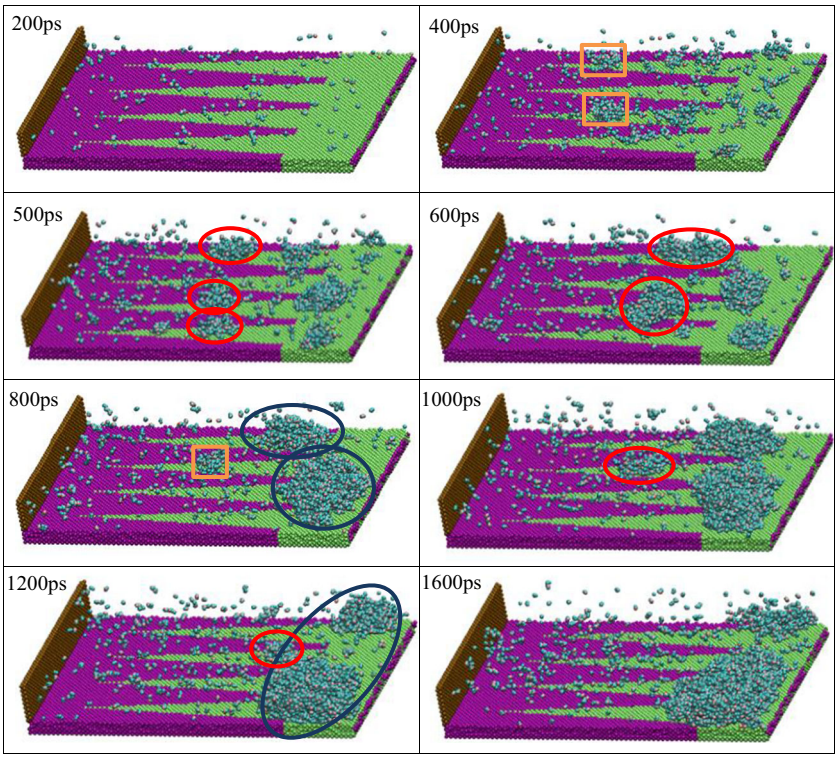

Fig. 3 Phenomena of water vapor condensation process without gravity ("□" represents cluster; "○" represents nuclei; "○" represents nano-droplet)

clusters continued to form and coalesce with each other on cold surfaces. ④ Condensation phenomena unchanged. From this moment, condensation process was nearly the same and the temperature of cold wall reached to the equilibrium. Finally, the temperature of hot wall was largest while it was smallest for cold wall. The temperature of water was in the middle. The result was in accordance with the law of energy conservation.

Effect of Different Gravity

Phenomena of Condensation Process

Gravity was a significant factor to affect the condensation rate. The condensation process with different gravity was depicted in Fig. 5. As described above on gravity of 0, the condensation first happened on vertex of V-shaped surface and the water

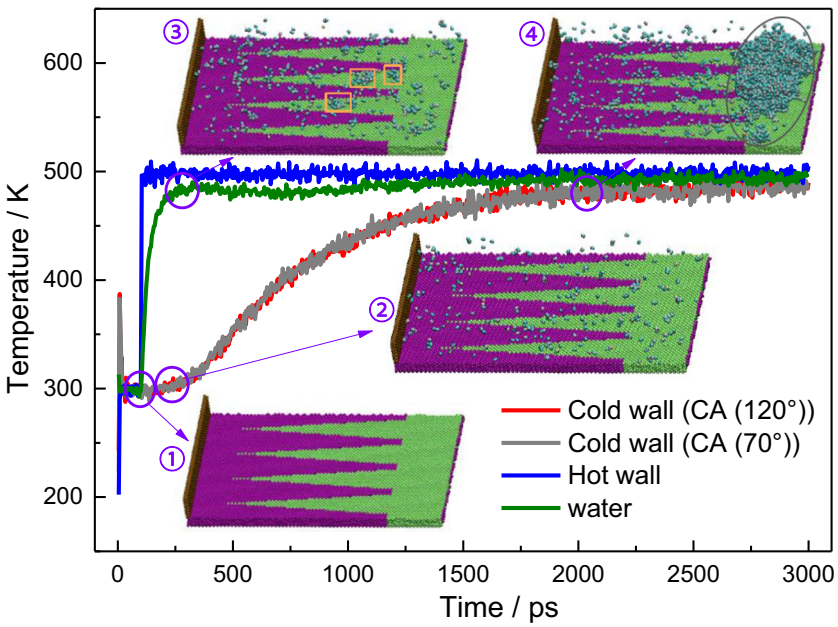

Fig. 4 Temperature of condensation process without gravity

Fig. 5 Phenomena of condensation process with different gravity

cluster or nuclei moved to the bottom with the increase of its volume. Finally, the nano-droplet formed on the bottom. When gravity was less than 0.003 kcal/(mol·Å), the phenomena was similar to the condition without gravity in spite of the increasing gravity. Since the gravity was not large enough, the water vapor molecules were still gradually condensed: Cluster or nuclei formed on vertex of V-shaped surface, then enlarged the volume and finally moved to the bottom. As the bottom of V-shaped surface was limited, the condensed water molecules coalesced to form a film. The final condensed water molecules

numbers and condensation rate increased with larger gravity, shown clearly in the figure. When gravity increased to 0.005 kcal/(mol·Å) or larger, the phenomena was quite different from the description before. As the gravity was large enough, the water liquid on hot wall dropped down massively and quickly condensed on cold wall. Especially in gravity of 0.01 kcal/(mol·Å), the whole cold wall was covered with water molecules. The condensation process was much quicker with greater gravity, leading to the larger condensation rate.

Numbers of Condensation Water Molecules

In order to describe the condensation rate more clearly, the numbers of condensation water molecules was calculated and depicted in Fig. 6. The numbers of condensation water molecules increased gradually over time, indicating the condensation process kept going. The condensation usually happened after 200 ps, except in $G = 0.01$ kcal/(mol·Å). In this case, the condensation happened quickly after 100 ps and nearly finished at 500 ps. In addition, the condensation finished at 1000 ps in $G = 0.005$ kcal/(mol·Å) and it was 1400 ps for other conditions. What's more, the slope of curve indicated the condensation rate directly. Therefore, it can be concluded that the condensation process was quicker with greater gravity. The final numbers of condensation water molecules was almost 3000 without gravity. It increased by 800 with gravity increased by 0.001 kcal/(mol·Å) when gravity was less than 0.002 kcal/(mol·Å). However, when gravity became to 0.003 kcal/(mol·Å), it increased by 3500, double of that without gravity. The final numbers of condensation water molecules couldn't increase indefinitely and it could only get close to 8340 with the larger gravity, limited by the total water molecules. Therefore, when gravity increased to 0.01 kcal/(mol·Å), an increasing gravity had little effect on the condensation process and condensation rate.

Temperature of Condensation Process

Variation of temperature and the condensation process was similar to each other when gravity was less than 0.003 kcal/(mol·Å). However, the condensation process was different when gravity was larger, shown in Fig. 7. ① The first key state point of temperature change during the condensation process was same to it without gravity, while the other three state points were different. At this moment, the temperature of hot wall was forced to increase to 498 K artificially to fulfill temperature difference between hot wall and cold wall for condensation. ② Partial water molecules separated from hot wall, but didn't contact cold wall. The condensation process and phenomena was quite different from it without gravity at this moment. The water molecules had already separated from hot wall like a "water column". It took time for "water column" to drop down and "water column" still stayed in the air during this period. Therefore, the temperature of cold wall at this state point was constant as well. While for condensation process without gravity, there was no "water column" formed and no clusters formed even if water vapor molecules began to contact cold wall. ③ Water molecules contacted cold wall. From this moment, the "water column" contacted the cold wall and transfer heat to cold wall quickly, leading to the increase of cold wall temperature. It only took 1000 ps for cold wall to reach equilibrium to finish the condensation, which was much shorter than 2000 ps without gravity. The results corresponded well with the discussion of condensation

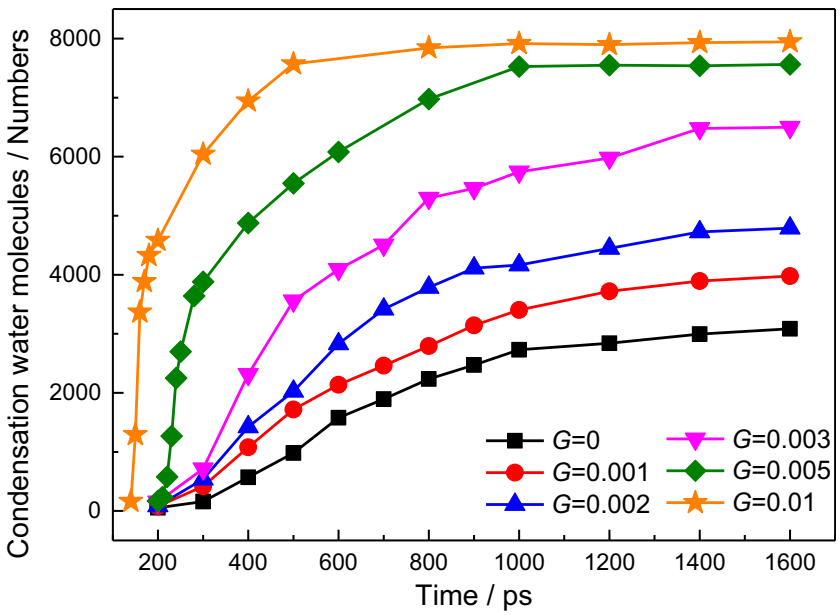

Fig. 6 Numbers of condensation water molecules with different gravity

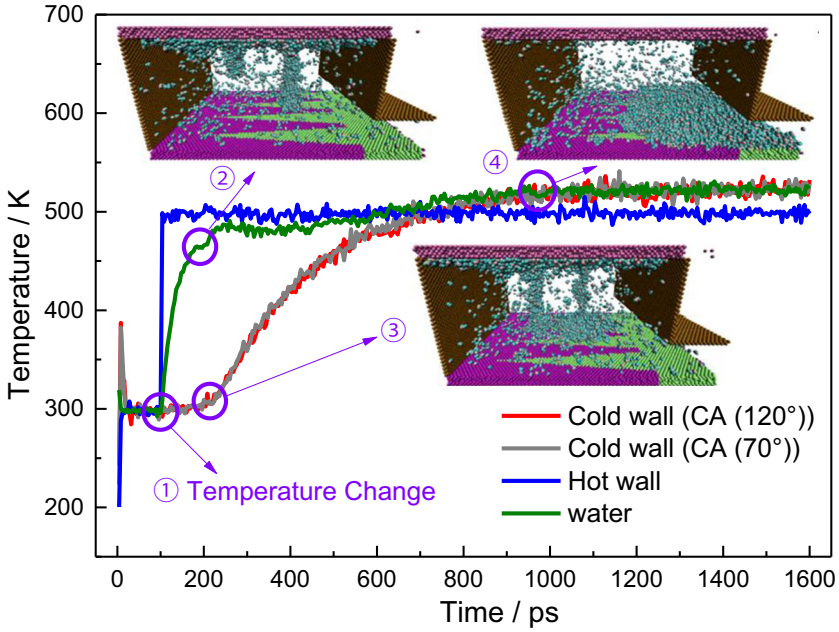

Fig. 7 Temperature of condensation process of G = 0.005 kcal/(mol·Å)

water molecule numbers. The water temperature continued to increase at this stage while it became to equilibrium without gravity. It was because the gravity potential will be transferred to thermal energy of water molecules and cold wall, which can be seen clearly in Fig. 9. ④ The final key state point was constant condensation phenomena. However, the temperature of hot wall was smallest, different from it without gravity. The temperature of water and cold wall were nearly the same. The reason was explained clearly in the next paragraph.

The average final temperature of cold wall, hot wall and water were obtained when condensation process stabilized, described in Fig. 8. The final temperature of cold wall and water was less than that of hot wall without gravity because there was no additional energy to increase thermal energy of water and cold wall. However, with the effect of gravity, the temperature of cold wall and water were larger than that of hot wall, especially for greater gravity. It was because the part of energy generated by gravity transferred to the thermal energy of water and cold wall, and the other part transferred to the kinetic energy of water. When gravity was less than 0.003 kcal/(mol·Å), the water vapor molecules continued to condense on cold wall and gravitational potential energy continued to transfer to thermal energy of water, leading to the temperature of water higher than that of cold wall.

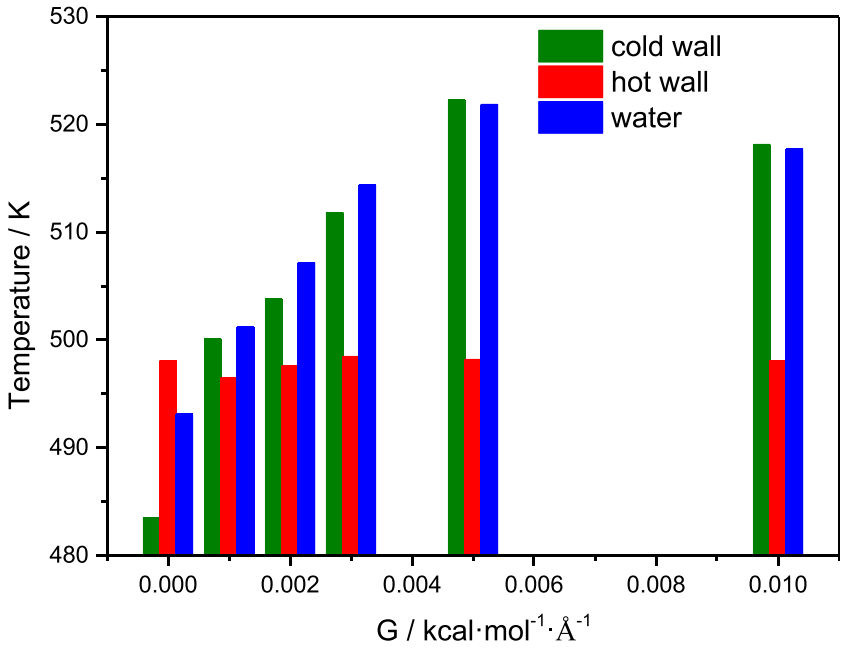

Fig. 8 The final temperature of condensation process with different gravity

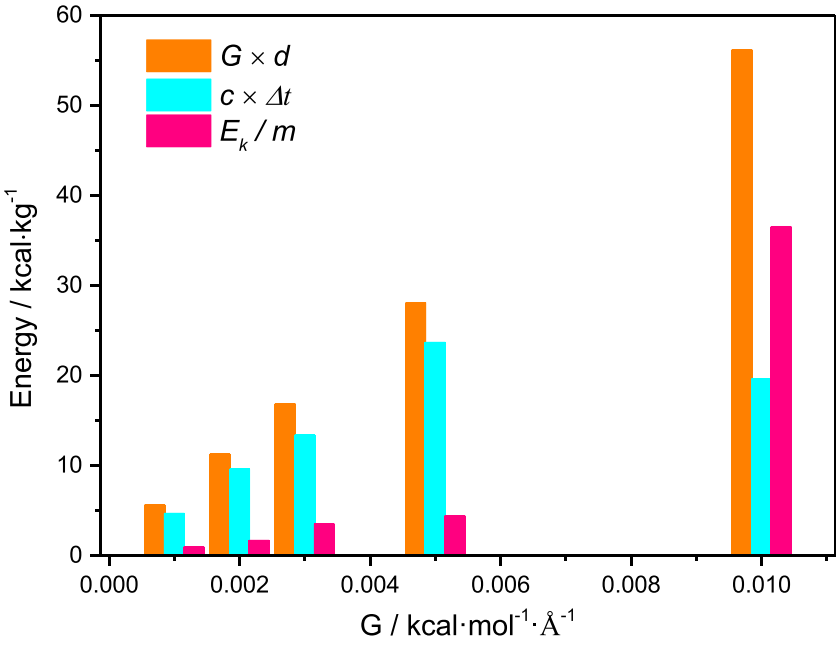

Fig. 9 The each term of energy with different gravity

Nevertheless, when gravity was larger than 0.005 kcal/(mol·Å), nearly all water vapor molecules condensed on cold wall finally and there was no more effect on water by gravity, resulting in the similar temperature between water and cold wall.

Energy of Condensation Process

When water molecules moved from hot wall to cold wall with the effect of gravity, the gravitational potential energy will transfer to thermal energy and kinetic energy of water molecules as followed:

$$E_p = E_t + E_k \tag{4}$$

Where E_p was gravitational potential energy, E_t was thermal energy and E_k was kinetic energy.

$$E_p = m \times G \times d \tag{5}$$

Where m was the mass of water molecules and d was the distance between hot wall and cold wall. The value of d was 101.08 Å.

$$E_t = c \times m \times \Delta t \tag{6}$$

Where c was specific heat capacity of water and its value was 1 kcal/(kg·°C). Δt was temperature difference.

In order to describe the change of E_k more clearly with the effect of gravity, the $\frac{E_k}{m}$ was obtained as followed:

$$\frac{E_k}{m} = G \times d - c \times \Delta t \tag{7}$$

The each term of eq. (7) was shown in Fig. 9. As can be seen, the gravitational potential energy and kinetic energy increased with greater gravity, while the thermal energy increased first and then decreased, corresponding well with the final temperature of condensation process with different gravity. It was because the water vapor molecules condensed on cold wall gradually when gravity was less than 0.005 kcal/(mol·Å) and gravitational potential energy could transferred more energy to thermal energy of water and cold wall. However, when gravity was 0.01 kcal/(mol·Å), the water molecules dropped down massively like a "water column" and impacted on cold wall. After then, the water molecules blasted around and most of gravitational potential energy transferred to kinetic energy of water. Therefore, the thermal energy of water and cold wall in this condition was less than it of 0.005 kcal/(mol·Å).

Conclusions

The model of water vapor condensation on a composite V-shaped surface with different gravity was built and the condensation process was studied by molecular dynamics. The numerical results indicated that the condensation mode could be controlled as a dropwise condensation with this model without gravity. What's more, the movement of condensate nano-droplet also could be controlled, which was helpful for increasing the efficiency of condensate drainage. The temperature of hot wall was largest while it was smallest for cold wall. The temperature of water was in the middle. The result was in accordance with the law of energy conservation. However, the

condensation process was different by the effect of gravity. It can be concluded that the condensation process was much quicker with greater gravity, leading to the larger condensation rate. The temperature of cold wall and water were larger than that of hot wall, especially for greater gravity. It was because the part of energy generated by gravity transferred to the thermal energy of water and cold wall, and the other part transferred to the kinetic energy of water. The gravitational potential energy and kinetic energy increased with greater gravity, while the thermal energy increased first and then decreased, corresponding well with the final temperature of condensation process with different gravity. Finally, the condensation mode could be controlled by the composite V-shaped surface with multi wettability gradients, accelerating the condensate drainage both with and without gravity, and providing a microcosmic mechanism and support for space experiment and provide guidance for component surface drainage of space system.

Acknowledgments This work was supported by National Natural Science Foundation of China [grant numbers 51676037] and ESA-CMSA International Cooperation of Space Experiment Project.

References

Alexiadis, A., Kassinos, S.: Molecular simulation of water in carbon nanotubes. Chem. Rev. **108**, 5014–5034 (2008)

Barisik, M., Beskok, A.: Boundary treatment effects on molecular dynamics simulations of interface thermal resistance. J. Comput. Phys. **231**, 7881–7892 (2012)

Chen, Y., Zheng, Y.: Bioinspired micro−/nanostructure fibers with a water collecting property. Nanoscale. **6**, 7703–7714 (2014)

Cheng, Y.T., Rodak, D.E., Angelopoulos, A., Gacek, R.: Microscopic observations of condensation of water on lotus leaves. Appl. Phys. Lett. **87**, 194112 (2005)

De Coninck, J., Blake, T.D.: Wetting and molecular dynamics simulations of simple liquids. Annu. Rev. Mater. Res. **38**, 1–22 (2008)

Diemand, J., Angélil, R., Tanaka, K.K., Tanaka, H.: Large scale molecular dynamics simulations of homogeneous nucleation. J. Chem. Phys. **139**, 074309 (2013)

ElSherbini, A.I., Jacobi, A.M.: A model for condensate retention on plain-fin heat exchangers. J Heat Trans-T ASME. **128**, 427–433 (2005)

Fu, T., Mao, Y., Tang, Y., Zhang, Y., Yuan, W.: Molecular dynamics simulation on rapid boiling of thin water films on cone-shaped nanostructure surfaces. Nanosc Microsc Therm. **19**, 17–30 (2015)

Gao, S., Liao, Q.W., Liu, W., Liu, Z.C.: Effects of solid fraction on droplet wetting and vapor condensation: a molecular dynamic simulation study. Langmuir. **33**, 12379–12388 (2017)

Gau, H., Herminghaus, S., Lenz, P., Lipowsky, R.: Liquid morphologies on structured surfaces: from microchannels to microchips. Science. **283**, 46–49 (1999)

D.O. Glushkov, J.C. Legros, P.A. Strizhak, R.S. Volkov. Heat and mass transfer at the ignition of vapors of volatile liquid fuels by hot metal core: Experimental study and modelling. 2016, 92:1182–1190

Hens, A., Agarwal, R., Biswas, G.: Nanoscale study of boiling and evaporation in a liquid Ar film on a Pt heater using molecular dynamics simulation. Int. J. Heat Mass Transf. **71**, 303–312 (2014)

Hoover, W.G.: Canonical dynamics: equilibrium phase-space distributions. Phys. Rev. A. **31**, 1695–1697 (1985)

Idem, S.A., Jacobi, A.M., Goldschmidt, V.W.: Fin heat transfer modeling and its impact on predictions of efficiency and condensation in gas-fired boilers. Heat Transfer Eng. **21**, 7–18 (2000)

Jung, J., Jang, E., Shoaib, M.A., Jo, K., Kim, J.S.: Droplet formation and growth inside a polymer network: a molecular dynamics simulation study. J. Chem. Phys. **144**, 134502 (2016)

Legros, J.C., Lutoshkina, O., Piskunov, M., Voytkov, I.: Water drops with graphite particles triggering the explosive liquid breakup. Exp. Thermal Fluid Sci. **96**, 154–161 (2018a)

Legros, J.C., Lutoshkina, O., Piskunov, M.: Vaporization of water droplets with non-metallic inclusions of different sizes in a high-temperature gas. Int. J. Therm. Sci. **127**, 360–372 (2018b)

Lei, Y.C., Chen, Z.Q., Shi, J.: Analysis of condensation heat transfer performance in curved triangle microchannels based on the volume of fluid method. Microgravity Sci Technol. **29**, 433–443 (2017)

Li, Z., Zhong, J.Q., Levin, D.A., Garrison, B.J.: Development of homogeneous water condensation models using molecular dynamics. AIAA J. **47**(5), 1241–1251 (2009)

Lin, S.P., Hudman, M.: Non-equilibrium evaporation and condensation at microgravity. Microgravity Sci Technol. **8**, 163–169 (1995)

Parker, A.R., Lawrence, C.W.: Water capture by a desert beetle. Nature. **414**, 33–34 (2001)

Plimpton, S.: Fast parallel algorithms for short-range molecular dynamics. J. Comput. Phys. **117**(1), 1–19 (1995)

Price, S.L., Stone, A.J., Alderton, M.: Explicit formulae for the electrostatic energy, forces and torques between a pair of molecules of arbitrary symmetry. Mol. Phys. **52**(4), 987–1001 (1984)

Pu, L., Li, H.X., Zhao, J.F., Chen, T.K.: Numerical simulation of condensation of bubbles under microgravity conditions by moving mesh method in the double-staggered grid. Microgravity Sci Technol. **21**, 15–22 (2009)

Seyf, H.R., Zhang, Y.: Effect of nanotextured array of conical features on explosive boiling over a flat substrate: a nonequilibrium molecular dynamics study. Int. J. Heat Mass Transf. **66**, 613–624 (2013)

Shi, M.H., Gan, Y.P., Ma, C.F.: Boiling and Condensation Heat Transfer, p. 305. Higher Education Press (1995)

Song, T.Y., Lan, Z., Ma, X.H., Bai, T.: Molecular clustering physical model of steam condensation and the experimental study on the initial droplet size distribution. Int. J. Therm. Sci. **48**, 2228–2236 (2009)

Toxværd, S.: Molecular dynamics simulation of heterogeneous nucleation at a structureless solid surface. J. Chem. Phys. **117**, 10303–10310 (2002)

Wolde, P.R., Frenkel, D.: Computer simulation study of gas-liquid nucleation in a Lennard-Jones system. J. Chem. Phys. **109**, 9901–9918 (1998)

Xu, B., Chen, Z.Q.: Droplet movement on a composite wedge-shaped surface with multi-gradients and different gravitational field by molecular dynamics. Microgravity Sci Technol. **30**(4), 571–579 (2018)

Xu, B., Chen, Z.Q.: Molecular dynamics study of water vapor condensation on a composite wedge-shaped surface with multi wettability gradients. Int Commun Heat Mass Transfer. **105**, 65–72 (2019)

Yasuoka, K., Matsumoto, M.: Molecular dynamics of homogeneous nucleation in the vapor phase I. Lennard-Jones fluid. J. Chem. Phys. **109**, 8451–8462 (1998a)

Yasuoka, K., Matsumoto, M.: Molecular dynamics of homogeneous nucleation in the vapor phase II. Water. J. Chem. Phys. **109**, 8463–8470 (1998b)

Yasuoka, K., Gao, G.T., Zeng, X.C.: Molecular dynamics simulation of supersaturated vapor nucleation in slit pore. J. Chem. Phys. **112**, 4279–4285 (2000)

Zhang, L.G., Shi, J., Xu, B., Chen, Z.Q.: Influences of pin geometry and inclination angle on condensation heat transfer performance of elliptical pin–fin surface. Microgravity Sci Technol. **30**, 1–10 (2018)

Zheng, Y.M., Han, D., Zhai, J., Jiang, L.: In situ investigation on dynamic suspending of microdroplet on lotus leaf and gradient of wettable micro- and nanostructure from water condensation. Appl. Phys. Lett. **92**, 084106 (2008)

Zheng, Y., Bai, H., Huang, Z., Tian, X., Nie, F., Zhao, Y., Zhai, J., Jiang, L.: Directional water collection on wetted spider silk. Nature. **463**, 640–643 (2010)

Publisher's Note Springer Nature remains neutral with regard to jurisdictional claims in published maps and institutional affiliations.